International Journal of Signal Processing, Image Processing and Pattern Recognition
Vol. 8, No. 5 (2015), pp. 55-74
http://dx.doi.org/10.14257/ijsip.2015.8.5.07

Implementation of 2-D Biorthogonal Wavelet Transform Using 2-D APDF

Qiming Fu, Xiao Zhou*, Chengyou Wang and Baochen Jiang

School of Mechanical, Electrical and Information Engineering, Shandong University, Weihai 264209, China
fqmsdu@163.com, zhouxiao@sdu.edu.cn, wangchengyou@sdu.edu.cn, jbc@sdu.edu.cn

Abstract

All phase digital filter (APDF) is a new type of linear phase FIR digital filter which was proposed in recent years, and a general method to design 2-D FIR digital filters called 2-D APDF is presented in this paper. Firstly, the theory of biorthogonal wavelet transform and 2-D APDF is expounded. Secondly, a novel algorithm is proposed to implement biorthogonal wavelet transform by using 2-D APDF based on DFT and IDCT. The relations between two kinds of filters are discussed. As an important application of biorthogonal wavelet transform, multi-resolution analysis of 2-D image signal could be used to test the feasibility and applicability of the proposed algorithm. Finally, the test image can be reconstructed perfectly in the multi-resolution analysis of 2-D image experiment using MATLAB tool in this paper, and the analysis indicates that the proposed method performs well.

Keywords: *DFT filtering, IDCT filtering, all phase digital filter (APDF), biorthogonal wavelet transform (BWT), Mallat algorithm*

1. Introduction

Digital filter design is an old but often changing topic. Over the last decade a number of researchers in digital signal processing have shown great interest in methods for designing digital filters. In order to avoid introducing the phase distortion in the signal processing and transmission, the phase shift of each frequency component in a signal through a system has to be proportional to its frequency. That is to say, the phase property of the system should be a straight line through the origin. Channels are required to have a linear phase property when images are processed or data is transmitted and FIR digital filter can be designed with strict linear phase property. Two-dimensional (2-D) FIR filters have important applications in image processing where the phase of the 2-D signal often needs to be preserved. Therefore, the design and realization of 2-D FIR filters have been received a great deal of attention. Conventional approaches to the design of such filters include the window method [1], in which a smoothing window is applied to the Fourier series coefficients of the ideal frequency response; the frequency transformation method [2], in which a one-dimensional (1-D) prototype filter response is mapped into a function of two frequency variables using an appropriate transformation function; the frequency sampling method [3], in which desired frequency response values are specified at certain sample points in the frequency domain.

In 2003, Hou, *et al.*, [4] proposed a concept of all phase data space. According to the DFT filtering theory, they also brought about the all phase digital filter (APDF) which was a new type of zero-phase filter. The APDF based on DFT method is a

ISSN: 2005-4254 IJSIP

new scheme for 1-D FIR filter design, possessing concurrently the merits of the window and the frequency sampling methods. It is superior to the conventional methods in overall filter characteristics. In 2004, Su, *et al.*, [5] proposed a method to design and implement APDF based on DCT. In 2006, Zhao, *et al.*, [6] proposed a better method in which they designed APDF based on DFT and IDCT through a simple transition matrix $\boldsymbol{G}$. This new method makes the process of designing APDF easier. On the basis of the above theory, a general method for designing 2-D APDF is presented in this paper.

Biorthogonal wavelet transform has played crucial roles in practical application, due to its lots of advantages as an important form of wavelet analysis. For example, the wavelet filter banks are symmetrical with compact support [7]. Now, biorthogonal wavelet transform has been used widely in the fields of image denoising [8, 9] and image coding [10]. In 1989, a pyramid algorithm was proposed by Mallat to implement fast wavelet transform (FWT) [11], and it is equivalent to the importance of FFT in Fourier transform. In 2013, Jiang, *et al.*, [12] proposed an algorithm to realize 1-D biorthogonal wavelet transform using all phase discrete cosine sequency filter (APDCSF). Since the image and computer vision information are two-dimensional, it is necessary to extend the wavelet theory from 1-D case to 2-D case. With analyzing the 2-D biorthogonal wavelet transform realized by 2-D Mallat algorithm and 2-D APDF, we propose a new algorithm to implement 2-D biorthogonal wavelet transform using 2-D APDF based on DFT and IDCT.

The rest of this paper is organized as follows. Section 2 starts with a brief review of biorthogonal wavelet transform. The method to design 2-D APDF is introduced in Section 3. Section 4 presents the algorithm designed to implement biorthogonal wavelet transform using 2-D APDF based on DFT and IDCT. The proposed method is tested by the typical image, and the experimental results are given in Section 5. Finally, conclusion and future work are given in Section 6.

2. Biorthogonal Wavelet Transform

Mathematically, the wavelet transform can be seen as the inner product of the original signal and the wavelet function (scaling function). Therefore, in the concrete realization, Daubechies proposed a calculation method by filter iteration. In the image decomposition and reconstruction, we can avoid introducing the phase distortion by using the wavelet function and scaling function with linear phase property. Phase distortion will lead to the distortion of the image edges and hence loss of important image content and therefore we need filters with symmetrical coefficient to achieve linear phase. None of the orthogonal wavelet systems, except Haar, has symmetrical coefficients. Biorthogonal wavelet system can be designed to achieve symmetry property and perfect reconstruction by using two scaling functions and two wavelet functions [13]. These two scaling functions ϕ and $\tilde{\phi}$ are used to produce different multiresolution analysis and correspondingly two wavelet functions ψ and $\tilde{\psi}$ are used in the analysis and synthesis respectively. The scaling functions ϕ , $\tilde{\phi}$ (wavelet functions ψ , $\tilde{\psi}$) are dual and orthogonal to each other, and this relationship is called biorthogonal [14].

2.1. One-dimensional Mallat Algorithm

The biorthogonal wavelet transform can be easily implemented using 1-D Mallat algorithm, which is shown in Figure 1. There are two pairs of sequences, ($\tilde{p}(n)$, $\tilde{q}(n)$) and ($p(n)$, $q(n)$). $\tilde{p}(n)$ and $\tilde{q}(n)$ are called decomposition sequences, $p(n)$ and $q(n)$ are called reconstruction sequences. The sliding inner product is

introduced in [15], which is equal to the convolution operation without time reversal procedure to original signal. Since decomposition and reconstruction sequences have symmetry property in the biorthogonal wavelet transform, 1-D Mallat algorithm can be realized by using 1-D filters.

What we can conclude from Figure 1 is that the essence of Mallat algorithm is filtering the signal $\{c_j(k)\}$ by decomposition filters $\tilde{p}(n)$ and $\tilde{q}(n)$ firstly. Then the results are down-sampled by factor 2. After the decomposition, the original signal is divided into two parts with the length which is equal to half of the original length. One part is the signal $\{c_{j-1}(k)\}$ generated by low-pass filter $\tilde{p}(n)$, which can be seen as the approximation of the original signal. And the other part is the signal $\{d_{j-1}(k)\}$ generated by high-pass filter $\tilde{q}(n)$, which can be seen as the detail of the original signal. On the other hand, the reconstruction process takes the reverse process to reconstruct the original signal by reconstruction filters $p(n)$ and $q(n)$.

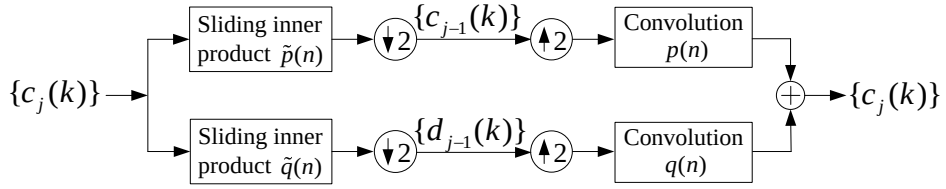

Figure 1. Implementation of 1-D Biorthogonal Wavelet Transform using Mallat Algorithm

The unit sample response of "CDF 9/7" ("bior4.4" in MATLAB) wavelet filters are

$$\tilde{p}(n) = [0.0378, -0.0238, -0.1106, 0.3774, 0.8527, 0.3774, -0.1106, -0.0238, 0.0378]^{\mathrm{T}},$$

$$n = -4, \cdots, -1, 0, 1, \cdots, 4;$$

$$\tilde{q}(n) = [-0.0645, 0.0407, 0.4181, -0.7885, 0.4181, 0.0407, -0.0645]^{\mathrm{T}},$$

$$n = -3, \cdots, -1, 0, 1, \cdots, 3;$$

$$p(n) = [-0.0645, -0.0407, 0.4181, 0.7885, 0.4181, -0.0407, -0.0645]^{\mathrm{T}},$$

$$n = -3, \cdots, -1, 0, 1, \cdots, 3;$$

$$q(n) = [-0.0378, -0.0238, 0.1106, 0.3774, -0.8527, 0.3774, 0.1106, -0.0238, -0.0378]^{\mathrm{T}},$$

$$n = -4, \cdots, -1, 0, 1, \cdots, 4.$$

2.2. Two-dimensional Mallat Algorithm

Furthermore, we generalize 1-D Mallat algorithm to 2-D Mallat algorithm using 2-D filters.

Figure 2 shows the implementation of 2-D discrete wavelet transform using 2-D Mallat algorithm. In Figure 2(a), filter the 2-D signal $\{c_j(k,l)\}$ using 2-D decomposition filters: low-pass filter $h(m,n)$, horizontal high-pass filter $g^{\mathrm{h}}(m,n)$, vertical high-pass filter $g^{\mathrm{v}}(m,n)$, and diagonal high-pass filter $g^{\mathrm{d}}(m,n)$. Then the filtering results conduct row down-sampled and column down-sampled by factor 2 in turn. After the decomposition, the original signal is divided into four subbands. One is the signal $\{c_{j-1}(k,l)\}$ generated by low-pass filter $h(m,n)$, which can be seen as low-frequency approximation of the original signal. The others are $\{d^{\mathrm{h}}_{j-1}(k,l)\}$, $\{d^{\mathrm{v}}_{j-1}(k,l)\}$ and $\{d^{\mathrm{d}}_{j-1}(k,l)\}$ generated by $g^{\mathrm{h}}(m,n)$, $g^{\mathrm{v}}(m,n)$ and $g^{\mathrm{d}}(m,n)$

respectively, which can be seen as high-frequency details of the original signal. On the contrary, the reconstruction process (Figure 2(b)) takes the reverse process to reconstruct the original 2-D signal using reconstruction filters: low-pass filter $\tilde{h}(m,n)$, horizontal high-pass filter $\tilde{g}^{\mathrm{h}}(m,n)$, vertical high-pass filter $\tilde{g}^{\mathrm{v}}(m,n)$, and diagonal high-pass filter $\tilde{g}^{\mathrm{d}}(m,n)$.

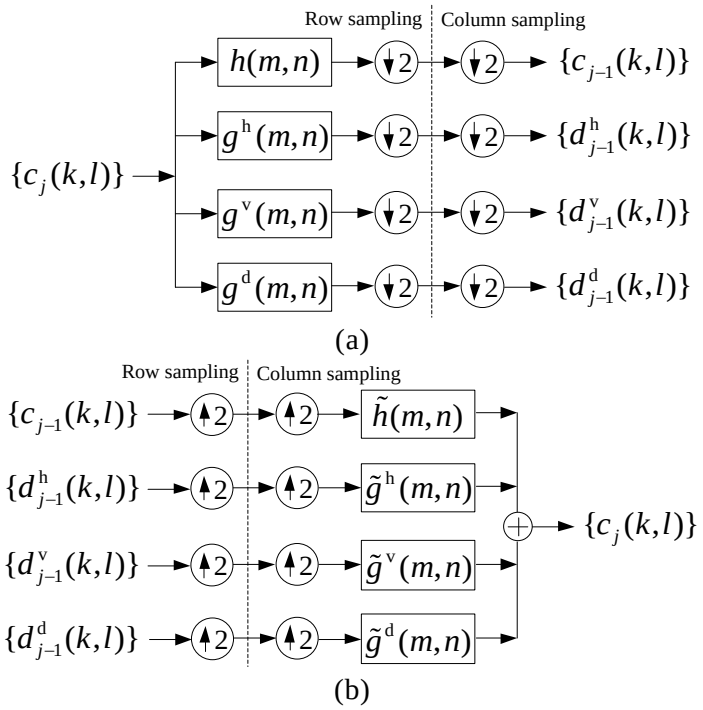

Figure 2. Implementation of 2-D Biorthogonal Wavelet Transform using 2-D Mallat Algorithm: (a) Decomposition Process, (b) Reconstruction Process

This paper selects biorthogonal wavelet "CDF 9/7" as an example to explain the process of transform. The unit sample response of each 2-D decomposition and reconstruction filters can be calculated by (1) and (2).

$$\begin{cases} h(m,n) = \tilde{p}(m)\tilde{p}(n), \ m,n = -4,\cdots,-1,0,1,\cdots,4, \\ g^{\mathrm{h}}(m,n) = \tilde{p}(m)\tilde{q}(n), \ m = -4,\cdots,-1,0,1,\cdots,4, \ n = -3,\cdots,-1,0,1,\cdots,3, \\ g^{\mathrm{v}}(m,n) = \tilde{q}(m)\tilde{p}(n), \ m = -3,\cdots,-1,0,1,\cdots,3, \ n = -4,\cdots,-1,0,1,\cdots,4, \\ g^{\mathrm{d}}(m,n) = \tilde{q}(m)\tilde{q}(n), \ m,n = -3,\cdots,-1,0,1,\cdots,3. \end{cases} \quad (1)$$

$$\begin{cases} \tilde{h}(m,n) = p(m)p(n), \ m,n = -3,\cdots,-1,0,1,\cdots,3, \\ \tilde{g}^{\mathrm{h}}(m,n) = p(m)q(n), \ m = -3,\cdots,-1,0,1,\cdots,3, \ n = -4,\cdots,-1,0,1,\cdots,4, \\ \tilde{g}^{\mathrm{v}}(m,n) = q(m)p(n), \ m = -4,\cdots,-1,0,1,\cdots,4, \ n = -3,\cdots,-1,0,1,\cdots,3, \\ \tilde{g}^{\mathrm{d}}(m,n) = q(m)q(n), \ m,n = -4,\cdots,-1,0,1,\cdots,4. \end{cases} \quad (2)$$

3. The Method to Design 2-D APDF Based on DFT

3.1. The Principle of All Phase Digital Filter (APDF) Based on DFT

All phase philosophy can be considered to an application of overlap philosophy [4, 16]. For a digital sequence $\{x(n)\}$, there are N N-D vectors. Each vector contains $x(n)$ and has different intercept phases:

$$\begin{aligned}
&\boldsymbol{X}_0 = [x(n), x(n+1), \cdots, x(n+N-2), x(n+N-1)]^{\mathrm{T}},\\
&\boldsymbol{X}_1 = z^{-1}\boldsymbol{X}_0 = [x(n-1), x(n), \cdots, x(n+N-3), x(n+N-2)]^{\mathrm{T}},\\
&\qquad\qquad\vdots\\
&\boldsymbol{X}_{N-1} = z^{-(N-1)}\boldsymbol{X}_0 = [x(n-N+1), x(n-N+2), \cdots, x(n-1), x(n)]^{\mathrm{T}},
\end{aligned} \tag{3}$$

where z^{-j} ($j = 0,1,\cdots,N-1$) stands for the delay operator. Obviously, $x(n)$ is the intersection of $\boldsymbol{X}_i (i = 0,1,\cdots,N-1)$, that is $x(n) = \boldsymbol{X}_0 \cap \boldsymbol{X}_1 \cap \cdots \cap \boldsymbol{X}_{N-1}$. According to the regular representation of data matrices, the all phase data matrix of $x(n)$ is defined as $\boldsymbol{X}_{-N+1,0}(n) = [\boldsymbol{X}_0, \boldsymbol{X}_1, \cdots, \boldsymbol{X}_{N-1}]$, and all the column vectors $\boldsymbol{X}_i (i = 0,1,\cdots,N-1)$ span an all phase data space of $x(n)$ [17].

We carry on filtering processing to each column vector $\boldsymbol{X}_i (i = 0,1,\cdots,N-1)$ in the all phase data matrix $\boldsymbol{X}_{-N+1,0}(n)$ of $x(n)$, and the output filtering results are N different vectors $\boldsymbol{Y}_l (l = 0,1,\cdots,N-1,)$:

$$\boldsymbol{Y}_l(i) = \frac{1}{N}\sum_{k=0}^{N-1} \boldsymbol{T}_N^{-1}(i,k)[\boldsymbol{F}_N(k)\sum_{j=0}^{N-1} \boldsymbol{T}_N(k,j)\boldsymbol{X}_l(j)] = \sum_{j=0}^{N-1} \boldsymbol{H}_N(i,j)\boldsymbol{X}_l(j),\ i,l = 0,1,\cdots,N-1, \tag{4}$$

where

$$\boldsymbol{H}_N(i,j) = \frac{1}{N}\sum_{k=0}^{N-1} \boldsymbol{T}_N^{-1}(i,k)\boldsymbol{T}_N(k,j)\boldsymbol{F}_N(k),\ i,j = 0,1,\cdots,N-1, \tag{5}$$

where $\boldsymbol{T}_N$ and $\boldsymbol{T}_N^{-1}$ denote the $N \times N$ transformation and inverse transformation matrix respectively. $\boldsymbol{F}_N$ is the N-D filter sequency response vector we expect, $\boldsymbol{F}_N = [F_N(0), F_N(1), \cdots, F_N(N-1)]^{\mathrm{T}}$. In the N different output vectors $\boldsymbol{Y}_l (l = 0,1,\cdots,N-1)$, we can get N different filtering values $\boldsymbol{Y}_l(l),\ l = 0,1,\cdots,N-1$, which corresponds to input value $x(n)$ respectively. To eliminate the ambiguity of filtering values caused by different intercept phases, the mean of these N filtering values $\boldsymbol{Y}_l(l),\ l = 0,1,\cdots,N-1$ is regarded as the filtering output of $x(n)$, that is:

$$y(n) = \frac{1}{N}\sum_{l=0}^{N-1} \boldsymbol{Y}_l(l) = \frac{1}{N}\sum_{l=0}^{N-1}\sum_{j=1}^{N-1} \boldsymbol{H}_N(l,j)x(n-l+j) = \sum_{\tau=-(N-1)}^{N-1} \boldsymbol{h}_N(\tau)x(n-\tau) = \boldsymbol{h}_N(n) * x(n), \tag{6}$$

where $\boldsymbol{h}_N(n) = [h_N(-N+1), \cdots, h_N(-1), h_N(0), h_N(1), \cdots, h_N(N-1)]^{\mathrm{T}}$ is the unit sample response of APDF.

$$\boldsymbol{h}_N(n) = \begin{cases} \dfrac{1}{N}\displaystyle\sum_{l=n}^{N-1} \boldsymbol{H}_N(l, l-n), & n = 0,1,\cdots,N-1,\\ \dfrac{1}{N}\displaystyle\sum_{l=0}^{N-1+n} \boldsymbol{H}_N(l, l-n), & n = -1,-2,\cdots,-N+1. \end{cases} \tag{7}$$

Architecture of the APDF based on DFT implemented directly in frequency domain is shown in Figure 3 [4].

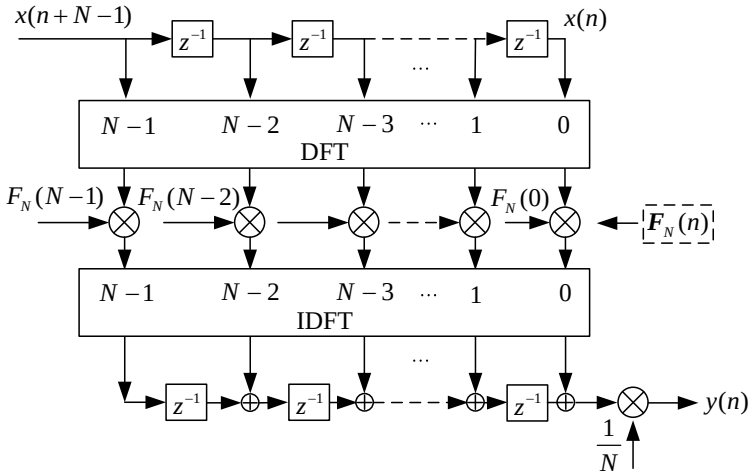

Figure 3. Architecture of the APDF based on DFT Implemented Directly in Frequency Domain

If transformation matrix $\boldsymbol{T}_N$ is DFT transformation matrix, the 1-D filter designed using this method is called APDF based on DFT. On the other hand, if transformation matrix $\boldsymbol{T}_N$ is IDCT transformation matrix, the 1-D filter designed using this method is called APDF based on IDCT. $\boldsymbol{f}_N$ denotes the inverse transform of the sequency response vector $\boldsymbol{F}_N$, that is $\boldsymbol{f}_N = \boldsymbol{T}_N^{-1}\boldsymbol{F}_N$, $\boldsymbol{f}_N = [f_N(0), f_N(1), \cdots, f_N(N-1)]^{\mathrm{T}}$. In APDF based on DFT, $\boldsymbol{f}_N$ is the IDFT of the frequency (sequency) response vector $\boldsymbol{F}_N$, and in APDF based on IDCT, $\boldsymbol{f}_N$ is the DCT of the sequency response vector $\boldsymbol{F}_N$.

Theorem 1: When N-D vector $\boldsymbol{F}_N$ is conjugate symmetric, $\boldsymbol{F}_N(n) = \boldsymbol{F}_N^*(N-n),\ n = 1,2;\cdots,N-1$, the APDF based on DFT filtering can be implemented by a zero-phase digital filter, whose unit sample response $\boldsymbol{h}_N(n)$ can be calculated by (8) [4].

$$\begin{cases} \boldsymbol{h}_N(n) = \dfrac{N-n}{N}\mathrm{IDFT}[\boldsymbol{F}_N(k)] = \dfrac{N-n}{N} f_N(n) \\ \boldsymbol{h}_N(-n) = \boldsymbol{h}_N(n) \end{cases}, \quad n,k = 0,1,\cdots,N-1. \tag{8}$$

From Theorem 1, a zero-phase 1-D filter can be designed using the APDF based on DFT method. This kind of filter is called APDF based on DFT.

Theorem 2: The APDF based on IDCT filtering can be implemented by a zero-phase digital filter, whose unit sample response $\boldsymbol{h}_N(n)$ can be calculated by (9) [18].

$$\begin{cases} \boldsymbol{h}_N(0) = \dfrac{1}{\sqrt{N}} f_N(0), \\ \boldsymbol{h}_N(n) = \dfrac{1}{N\sqrt{N}}\left(1 + \dfrac{N-n-1}{\sqrt{2}}\right) f_N(n),\ n = 1,2,\cdots,N-1, \\ \boldsymbol{h}_N(-n) = \boldsymbol{h}_N(n),\ n = 1,2,\cdots,N-1. \end{cases} \tag{9}$$

From Theorem 2, a zero-phase 1-D filter can be designed using the APDF based on IDCT method. This kind of filter is called APDF based on IDCT.

3.2. Derivation of Transition Matrix $\boldsymbol{G}_N$

According to (8) and (9), in [6], $\boldsymbol{h}_N$ can be expressed as:

$$[\boldsymbol{h}_{1/2}]_N = \boldsymbol{D}_N \boldsymbol{f}_N = \boldsymbol{D}_N \boldsymbol{T}_N^{-1} \boldsymbol{F}_N = \boldsymbol{G}_N \boldsymbol{F}_N, \tag{10}$$

where $[\boldsymbol{h}_{1/2}]_N = [h_N(0), h_N(1), \cdots, h_N(N-1)]^{\mathrm{T}}$, and $\boldsymbol{G}_N$ is called transition matrix, which size is $N \times N$, and $\boldsymbol{G}_N = \boldsymbol{D}_N \boldsymbol{T}_N^{-1}$. $\boldsymbol{D}_N$ is called the diagonal weighting matrix.

One step further, $\boldsymbol{F}_N$ can be obtained easily when we know unit sample response $\boldsymbol{h}_N$. According to (10), we have

$$\boldsymbol{F}_N = \boldsymbol{G}_N^{-1} [\boldsymbol{h}_{1/2}]_N, \tag{11}$$

where $\boldsymbol{G}_N^{-1} = \boldsymbol{T}_N \boldsymbol{D}_N^{-1}$. $\boldsymbol{G}_N^{-1}$ is the inverse matrix of $\boldsymbol{G}_N$, which size is $N \times N$.

(10) and (11) have established a conversion relation between unit sample response $\boldsymbol{h}_N$ and *N*-D filter sequency response vector $\boldsymbol{F}_N$ by transition matrix $\boldsymbol{G}_N$ and inverse transition matrix $\boldsymbol{G}_N^{-1}$.

In APDF based on DFT design, $\boldsymbol{T}_N^{-1}$ stands for IDFT matrix, and $\boldsymbol{T}_N$ is DFT matrix. $\boldsymbol{T}_N^{-1}(m,n) = \frac{1}{N} W_N^{-m \times n}$, where $W_N = \mathrm{e}^{-\mathrm{j}\frac{2\pi}{N}}$. We denote the transition matrix in APDF based on DFT design as $[\boldsymbol{G}_N]_{\mathrm{DFT}}$ and the cell (m,n) in the $[\boldsymbol{G}_N]_{\mathrm{DFT}}$ can be expressed as:

$$[\boldsymbol{G}_N(m,n)]_{\mathrm{DFT}} = \frac{N-m}{N^2} W_N^{-m \times n}, \ m,n = 0,1,\cdots,N-1. \tag{12}$$

And the inverse matrix of $[\boldsymbol{G}_N]_{\mathrm{DFT}}$ can be expressed as:

$$\left[\boldsymbol{G}_N^{-1}(m,n)\right]_{\mathrm{DFT}} = \frac{N}{N-n} W_N^{m \times n}, \ m,n = 0,1,\cdots,N-1. \tag{13}$$

In APDF based on IDCT design, $\boldsymbol{T}_N^{-1}$ stands for DCT matrix, and $\boldsymbol{T}_N$ is IDCT matrix. We denote the transition matrix in APDF based on IDCT design as $[\boldsymbol{G}_N]_{\mathrm{IDCT}}$ and the cell (m,n) in the $[\boldsymbol{G}_N]_{\mathrm{IDCT}}$ can be expressed as:

$$[\boldsymbol{G}_N(m,n)]_{\mathrm{IDCT}} = \begin{cases} \dfrac{1}{N}, & m = 0, n = 0,1,\cdots,N-1, \\ \dfrac{N-m+\sqrt{2}-1}{N^2} \cos\dfrac{(2n+1)m\pi}{2N}, & m = 1,2,\cdots,N-1, n = 0,1,\cdots,N-1. \end{cases} \tag{14}$$

Since $[\boldsymbol{G}_N]_{\mathrm{IDCT}}$ is an orthogonal matrix, the inverse matrix of $[\boldsymbol{G}_N]_{\mathrm{IDCT}}$ is the transposition of matrix $[\boldsymbol{G}_N]_{\mathrm{IDCT}}$:

$$\left[\boldsymbol{G}_N^{-1}(m,n)\right]_{\mathrm{IDCT}} = \left[\boldsymbol{G}_N^{\mathrm{T}}(m,n)\right]_{\mathrm{IDCT}}, \tag{15}$$

$$\left[\boldsymbol{G}_N^{-1}(m,n)\right]_{\mathrm{IDCT}} = \begin{cases} 1, & n = 0, \ m = 0,1,\cdots,N-1, \\ \dfrac{2N}{N-n+\sqrt{2}-1} \cos\dfrac{(2m+1)n\pi}{2N}, & n = 1,2,\cdots,N-1, \ m = 0,1,\cdots,N-1. \end{cases} \tag{16}$$

3.3. The Method to Design a 2-D APDF Based on DFT Using Transition Matrix

The design formulas of the 1-D APDF have been described in the Section 3.1 and Section 3.2. Hou [19, 20] proposed the expression of 2-D APDF based on DCT but didn't give a general design method. This part will represent the design method of 2-D APDF.

According to (10), we generalize 1-D APDF to 2-D APDF using $\boldsymbol{G}_N$ and its transposed matrix $\boldsymbol{G}_N^{\mathrm{T}}$:

$$[\boldsymbol{Q}_{1/4}]_{M\times N} = \boldsymbol{G}_M \boldsymbol{F}_{M\times N} \boldsymbol{G}_N^{\mathrm{T}}, \tag{17}$$

where $[\boldsymbol{Q}_{1/4}]_{M\times N}$ is located in the lower right corner of $\boldsymbol{Q}$ which size is $(2M-1)\times(2N-1)$, and $\boldsymbol{Q}$ is the unit sample response of the 2-D filter called 2-D APDF. $\boldsymbol{G}_M$ ($\boldsymbol{G}_N$) is the transition matrix, and the sizes of $\boldsymbol{G}_M$ and $\boldsymbol{G}_N$ are $M\times M$ and $N\times N$ respectively. $\boldsymbol{G}_N^{\mathrm{T}}$ is the transposed matrix of $\boldsymbol{G}_N$. $\boldsymbol{F}_{M\times N}$ is the filter sequency response matrix.

Theorem 3: The 2-D APDF has zero phase characteristic, whose unit sample response $\boldsymbol{Q}$ can be obtained by symmetry in the horizontal and vertical directions [19, 20]. That is

$$\boldsymbol{Q}(m,n) = \boldsymbol{Q}(-m,n) = \boldsymbol{Q}(m,-n) = \boldsymbol{Q}(-m,-n),\ m = 0,1,\cdots,M-1,\ n = 0,1,\cdots,N-1. \tag{18}$$

According to Theorem 3, the unit sample response of 2-D APDF $\boldsymbol{Q}$ can be easily obtained by calculating $[\boldsymbol{Q}_{1/4}]_{M\times N}$,

$$[\boldsymbol{Q}_{1/4}]_{M\times N} = \begin{bmatrix} Q(0,0) & Q(0,1) & \cdots & Q(0,N-1) \\ Q(1,0) & Q(1,1) & \cdots & Q(1,N-1) \\ \cdots & \cdots & \ddots & \vdots \\ Q(M-1,0) & Q(M-1,1) & \cdots & Q(M-1,N-1) \end{bmatrix}. \tag{19}$$

With unit sample response $\boldsymbol{Q}$, 2-D APDF filtering can be implemented using 2-D convolution method shown as (20).

$$y(m,n) = \sum_{k_1=-M}^{M} \sum_{k_2=-N}^{N} \boldsymbol{Q}(k_1,k_2) u(m-k_1, n-k_2), \tag{20}$$

where $y(m,n)$, $u(m,n)$ are the output and input 2-D signals of 2-D APDF respectively.

From preceding analysis, a zero-phase 2-D filter can be designed using the 2-D APDF method. This kind of filter is called 2-D APDF.

In APDF based on DFT design,

$$[\boldsymbol{Q}_{1/4}]_{M\times N} = [\boldsymbol{G}_M]_{\mathrm{DFT}} [\boldsymbol{F}_{M\times N}]_{\mathrm{DFT}} \left[\boldsymbol{G}_N^{\mathrm{T}}\right]_{\mathrm{DFT}}. \tag{21}$$

In APDF based on IDCT design,

$$[\boldsymbol{Q}_{1/4}]_{M\times N} = [\boldsymbol{G}_M]_{\mathrm{IDCT}} [\boldsymbol{F}_{M\times N}]_{\mathrm{IDCT}} \left[\boldsymbol{G}_N^{\mathrm{T}}\right]_{\mathrm{IDCT}}. \tag{22}$$

3.4. 2-D APDF Filtering Realized in Transform Domain

All phase philosophy can be considered to an application of overlap philosophy, which is used in 2-D APDF. For a pixel in 2-D signal matrix, there are $M\times N$

blocks that contain the pixel in the spatial domain and each block has different intercept phases. The case ($M = 2, N = 2$) is described in Figure 4.

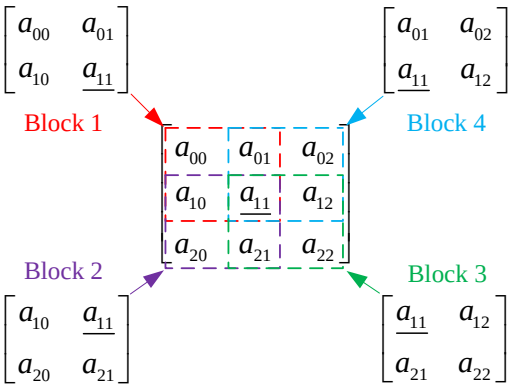

Figure 4. $M \times N$ **Blocks that Contain the Pixel** a_{11} **in the Spatial Domain (** $M = 2, N = 2$ **)**

Every block containing the pixel has been taken into consideration for reducing the Gibbs effect, when the pixel in the 2-D signal matrix is filtered by 2-D APDF. Figure 5 describes the process of 2-D APDF filtering to a pixel in the 2-D signal transform domain.

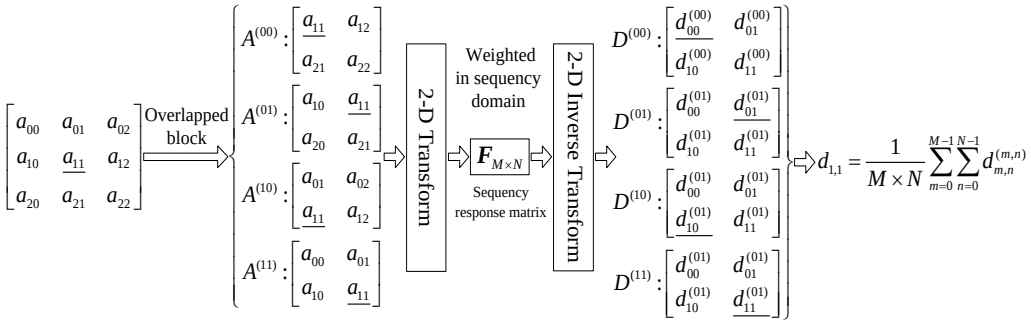

Figure 5. The Process of 2-D APDF Filtering to a Pixel in the 2-D Signal Matrix in Transform Domain ($M = 2, N = 2$ **)**

Thus, 2-D APDF filtering process can be realized in transform domain. And on the basis of the previous analysis, $(2M-1)\times(2N-1)$ pixels have been used when a pixel was filtered using 2-D APDF. Since all phase philosophy makes full use of the pixel correlation of adjacent block, the filtering performance is good certainly.

Theorem 4: For a 2N-1 order 1-D APDF based on DFT, the samples of the its transfer function $H(e^{j2\pi k/N})$ are equal to the values of the frequency response vector $\boldsymbol{F}_N(k)$. It means that the 1-D APDF based on DFT has the property of frequency sampling [4].

Compared with 1-D APDF based on IDCT [18], 1-D APDF based on DFT is especially significant in the case that the filter frequency response at frequency samples need to be controlled precisely [4]. With strictly inheriting the 1-D APDF based on DFT method, 2-D APDF based on DFT has the merit owned by 1-D APDF based on DFT.

4. Algorithm Design of Biorthogonal Wavelet Transform Using 2-D APDF

4.1. Process of 2-D Biorthogonal Wavelet Transform Using 2-D APDF

When applying 2-D Mallat algorithm to the finite length 2-D signal $\{c_j(m,n)\}$, the data beyond the sequence must be extended. Among various boundary extension methods, periodic extension is used frequently.

The 2-D APDF method is a new scheme for 2-D FIR filter design. We can use the novel method to design the 2-D decomposition filters and 2-D reconstruction filters in 2-D Mallat algorithm. Implementation of 2-D biorthogonal wavelet transform using 2-D APDF is shown in Figure 6.

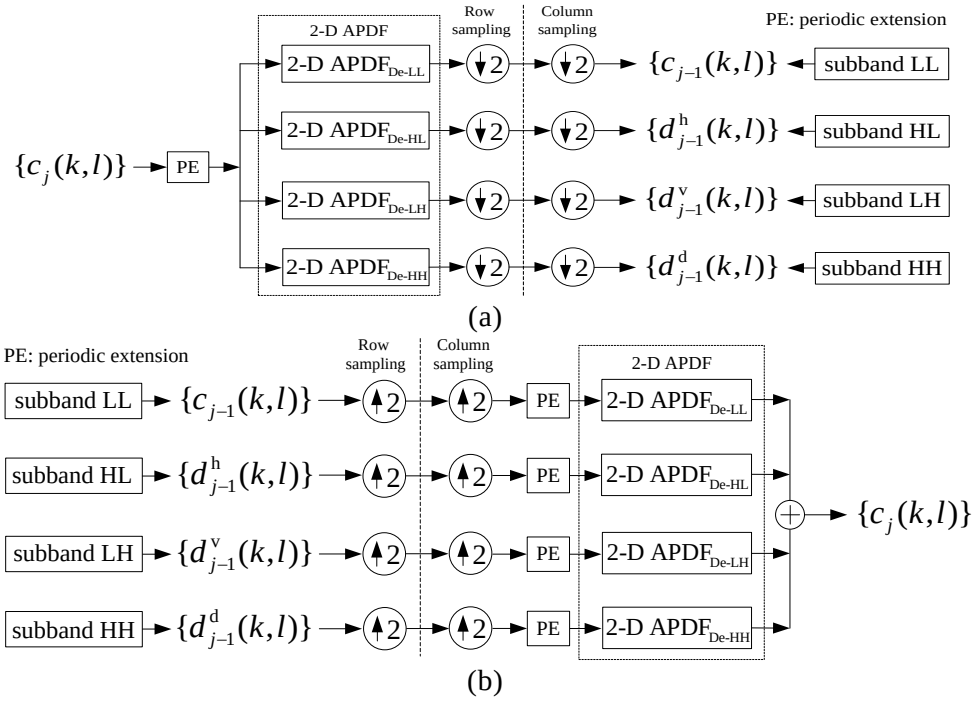

Figure 6. Implementation of 2-D Biorthogonal Wavelet Transform using 2-D APDF: (a) Decomposition Process, (b) Reconstruction Process

After 2-D biorthogonal wavelet decomposition to the image, four parts are derived: LL, HL, LH and HH. The distribution of wavelet coefficients after one layer 2-D biorthogonal wavelet transform (BWT) to an image is shown in Figure 7.

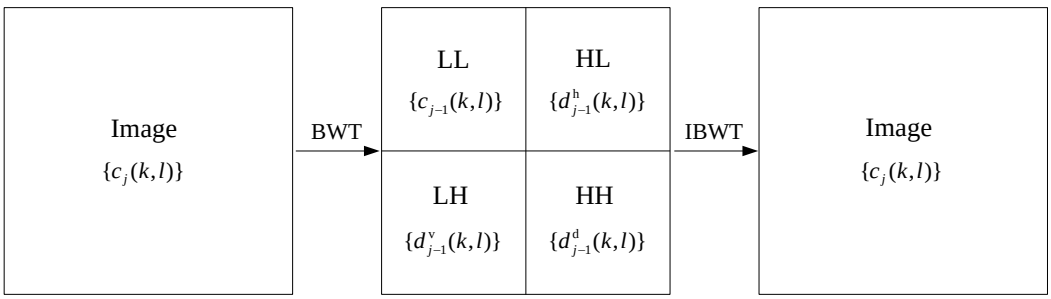

Figure 7. The Distribution of Wavelet Coefficients after One Layer 2-D Biorthogonal Wavelet Transform to Image

4.2. The Process of a 2-D Signal through the 2-D APDF Realized in Transform Domain

The process of a 2-D signal through the 2-D APDF is shown in Figure 8. $\boldsymbol{F}_{M\times N}$ is the sequency response matrix in the 2-D APDF. With the $\boldsymbol{F}_{M\times N}$, 2-D APDF filtering can be realized in transform domain. $\boldsymbol{F}_{\text{De-LL}}$, $\boldsymbol{F}_{\text{De-HL}}$, $\boldsymbol{F}_{\text{De-LH}}$, $\boldsymbol{F}_{\text{De-HH}}$ and $\boldsymbol{F}_{\text{Re-LL}}$, $\boldsymbol{F}_{\text{Re-HL}}$, $\boldsymbol{F}_{\text{Re-LH}}$, $\boldsymbol{F}_{\text{Re-HH}}$ are sequency response matrices corresponding to the 2-D APDF in Figure 6, and these 2-D APDF that have different characteristics in filtering are used to decompose and reconstruct in 2-D biorthogonal wavelet transform.

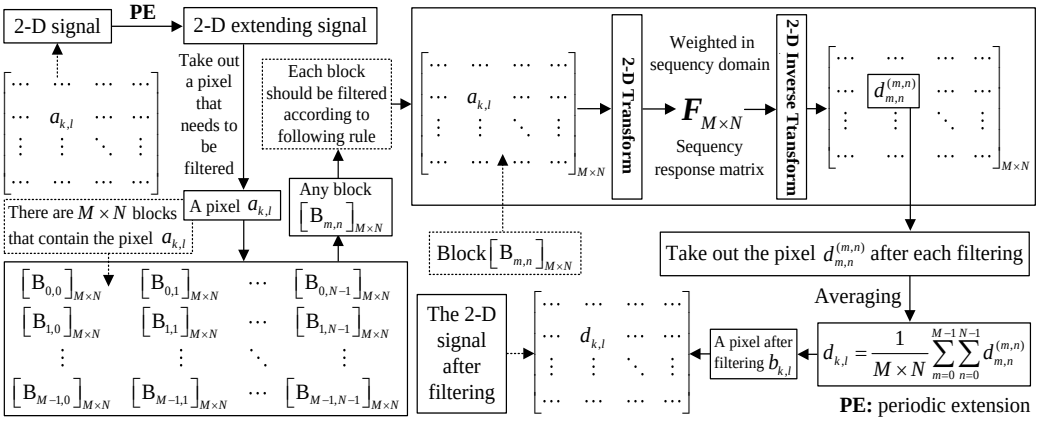

Figure 8. The Process of a 2-D Signal Through the 2-D APDF Realized in Transform Domain

Case 1: In 2-D APDF based on DFT filtering, 2-D transform and inverse transform in Figure 5, 8 are 2-D DFT and IDFT respectively, and frequency (sequency) response matrix is denoted as $[\boldsymbol{F}_{M\times N}]_{\text{DFT}}$.

Case 2: In 2-D APDF based on IDCT filtering, 2-D transform and inverse transform in Figure 5, 8 are 2-D IDCT and DCT respectively, and sequency response matrix is denoted as $[\boldsymbol{F}_{M\times N}]_{\text{IDCT}}$.

In summary, just let we know the eligible filter sequency response matrices $\boldsymbol{F}_{\text{De-LL}}$, $\boldsymbol{F}_{\text{De-HL}}$, $\boldsymbol{F}_{\text{De-LH}}$, $\boldsymbol{F}_{\text{De-HH}}$ and $\boldsymbol{F}_{\text{Re-LL}}$, $\boldsymbol{F}_{\text{Re-HL}}$, $\boldsymbol{F}_{\text{Re-LH}}$, $\boldsymbol{F}_{\text{Re-HH}}$, and then the 2-D biorthogonal wavelet transform can be realized using 2-D APDF.

4.3. Solving the Sequency Response Matrix in the 2-D APDF

If the unit sample response of 2-D filter were known, filter sequency response matrix $\boldsymbol{F}_{M\times N}$ we expect in the 2-D APDF can be obtained. That is

$$\boldsymbol{F}_{M\times N}=\boldsymbol{G}_M^{-1}[\boldsymbol{Q}_{1/4}]_{M\times N}(\boldsymbol{G}_N^{\mathrm{T}})^{-1}=\boldsymbol{G}_M^{-1}[\boldsymbol{Q}_{1/4}]_{M\times N}(\boldsymbol{G}_N^{-1})^{\mathrm{T}}. \tag{23}$$

With the unit sample response of each 2-D APDF known, each eligible filter sequency response matrix $\boldsymbol{F}_{\text{De-LL}}$, $\boldsymbol{F}_{\text{De-HL}}$, $\boldsymbol{F}_{\text{De-LH}}$, $\boldsymbol{F}_{\text{De-HH}}$ and $\boldsymbol{F}_{\text{Re-LL}}$, $\boldsymbol{F}_{\text{Re-HL}}$, $\boldsymbol{F}_{\text{Re-LH}}$, $\boldsymbol{F}_{\text{Re-HH}}$ can be obtained respectively according to (23).

However, there is a much simpler way to obtain the sequency response matrix in each 2-D APDF. From (1), (2), (11) and (23), we have

$$\begin{aligned}\boldsymbol{F}_{M\times N}(m,n) &= \sum_{k=0}^{M-1}\sum_{l=0}^{N-1}\boldsymbol{G}_M^{-1}(m,k)\left[\boldsymbol{Q}_{1/4}(k,l)\right]_{M\times N}\boldsymbol{G}_N^{-1}(n,l)\\ &= \sum_{k=0}^{M-1}\sum_{l=0}^{N-1}\boldsymbol{G}_M^{-1}(m,k)\left[\boldsymbol{h}_{1/2}^{'}(k)\right]_M\left[\boldsymbol{h}_{1/2}^{''}(l)\right]_N\boldsymbol{G}_N^{-1}(n,l)\\ &= \sum_{k=0}^{M-1}\boldsymbol{G}_M^{-1}(m,k)\left[\boldsymbol{h}_{1/2}^{'}(k)\right]_M\sum_{l=0}^{N-1}\boldsymbol{G}_N^{-1}(n,l)\left[\boldsymbol{h}_{1/2}^{''}(l)\right]_N\\ &= \boldsymbol{F}_M^{'}(m)\boldsymbol{F}_N^{''}(n),\end{aligned} \tag{24}$$

where $[\boldsymbol{Q}_{1/4}(k,l)]_{M\times N} = \left[\boldsymbol{h}_{1/2}^{'}(k)\right]_M\left[\boldsymbol{h}_{1/2}^{''}(l)\right]_N$, $\left[\boldsymbol{h}_{1/2}^{'}\right]_M = [h_M^{'}(0), h_M^{'}(1),\cdots, h_M^{'}(N-1)]^{\mathrm{T}}$, and $\left[\boldsymbol{h}_{1/2}^{''}\right]_N = [h_N^{''}(0), h_N^{''}(1),\cdots, h_N^{''}(N-1)]^{\mathrm{T}}$.

This paper selects biorthogonal wavelet "CDF 9/7" as an example to explain the process of solving the sequency response matrix in the 2-D APDF. A sequency response matrix $\boldsymbol{F}_{\text{De-LL}}$ is got by (25).

$$\begin{aligned}\boldsymbol{F}_{\text{De-LL}}(m,n) &= \sum_{k=0}^{3}\sum_{l=0}^{3}\boldsymbol{G}_4^{-1}(m,k)\left[h_{1/4}(k,l)\right]_{4\times 4}\boldsymbol{G}_4^{-1}(n,l)\\ &= \sum_{k=0}^{3}\sum_{l=0}^{3}\boldsymbol{G}_4^{-1}(m,k)\left[\tilde{p}_{1/2}(k)\right]_4\left[\tilde{p}_{1/2}(l)\right]_4\boldsymbol{G}_4^{-1}(n,l)\\ &= \sum_{k=0}^{3}\boldsymbol{G}_4^{-1}(m,k)\left[\tilde{p}_{1/2}(k)\right]_4\sum_{l=0}^{3}\boldsymbol{G}_4^{-1}(n,l)\left[\tilde{p}_{1/2}(l)\right]_4\\ &= \boldsymbol{F}_4^{\tilde{p}}(m)\boldsymbol{F}_4^{\tilde{p}}(n).\end{aligned} \tag{25}$$

$\boldsymbol{F}_{\text{De-HL}}$, $\boldsymbol{F}_{\text{De-LH}}$, $\boldsymbol{F}_{\text{De-HH}}$ and $\boldsymbol{F}_{\text{Re-LL}}$, $\boldsymbol{F}_{\text{Re-HL}}$, $\boldsymbol{F}_{\text{Re-LH}}$, $\boldsymbol{F}_{\text{Re-HH}}$ can be got in the same way.

$$\begin{cases}\boldsymbol{F}_{\text{De-LL}}(m,n) = \boldsymbol{F}_4^{\tilde{p}}(m)\boldsymbol{F}_4^{\tilde{p}}(n), & \boldsymbol{F}_{\text{De-HL}}(m,n) = \boldsymbol{F}_4^{\tilde{p}}(m)\boldsymbol{F}_3^{\tilde{q}}(n),\\ \boldsymbol{F}_{\text{De-LH}}(m,n) = \boldsymbol{F}_3^{\tilde{q}}(m)\boldsymbol{F}_4^{\tilde{p}}(n), & \boldsymbol{F}_{\text{De-HH}}(m,n) = \boldsymbol{F}_3^{\tilde{q}}(m)\boldsymbol{F}_3^{\tilde{q}}(n).\end{cases} \tag{26}$$

$$\begin{cases}\boldsymbol{F}_{\text{Re-LL}}(m,n) = \boldsymbol{F}_3^{p}(m)\boldsymbol{F}_3^{p}(n), & \boldsymbol{F}_{\text{Re-HL}}(m,n) = \boldsymbol{F}_3^{p}(m)\boldsymbol{F}_4^{q}(n),\\ \boldsymbol{F}_{\text{Re-LH}}(m,n) = \boldsymbol{F}_4^{q}(m)\boldsymbol{F}_3^{p}(n), & \boldsymbol{F}_{\text{Re-HH}}(m,n) = \boldsymbol{F}_4^{q}(m)\boldsymbol{F}_4^{q}(n).\end{cases} \tag{27}$$

As discussed above, sequency response matrices $\boldsymbol{F}_{\text{De-LL}}$, $\boldsymbol{F}_{\text{De-HL}}$, $\boldsymbol{F}_{\text{De-LH}}$, $\boldsymbol{F}_{\text{De-HH}}$ and $\boldsymbol{F}_{\text{Re-LL}}$, $\boldsymbol{F}_{\text{Re-HL}}$, $\boldsymbol{F}_{\text{Re-LH}}$, $\boldsymbol{F}_{\text{Re-HH}}$ could be easily obtained, if sequency response vectors $\boldsymbol{F}_4^{\tilde{p}}$, $\boldsymbol{F}_3^{\tilde{q}}$, $\boldsymbol{F}_3^{p}$ and $\boldsymbol{F}_4^{q}$ were known. From (11) and (25), we have

$$\begin{cases}\boldsymbol{F}_4^{\tilde{p}} = \boldsymbol{G}_4^{-1}\left[\tilde{p}_{1/2}\right]_4, & \boldsymbol{F}_3^{\tilde{q}} = \boldsymbol{G}_3^{-1}\left[\tilde{q}_{1/2}\right]_3,\\ \boldsymbol{F}_3^{p} = \boldsymbol{G}_3^{-1}\left[p_{1/2}\right]_3, & \boldsymbol{F}_4^{q} = \boldsymbol{G}_4^{-1}\left[q_{1/2}\right]_4.\end{cases} \tag{28}$$

If filter sequency response vectors $\boldsymbol{F}_4^{\tilde{p}}$, $\boldsymbol{F}_3^{\tilde{q}}$, $\boldsymbol{F}_3^{p}$ and $\boldsymbol{F}_4^{q}$ were provided, every 2-D APDF in Figure 6 can be realized in transform domain, and then biorthogonal wavelet transform can be implemented by using these 2-D APDF. The filter sequency response vectors and matrices corresponding to the 2-D APDF in 2-D biorthogonal wavelet transform is shown in Figure 9.

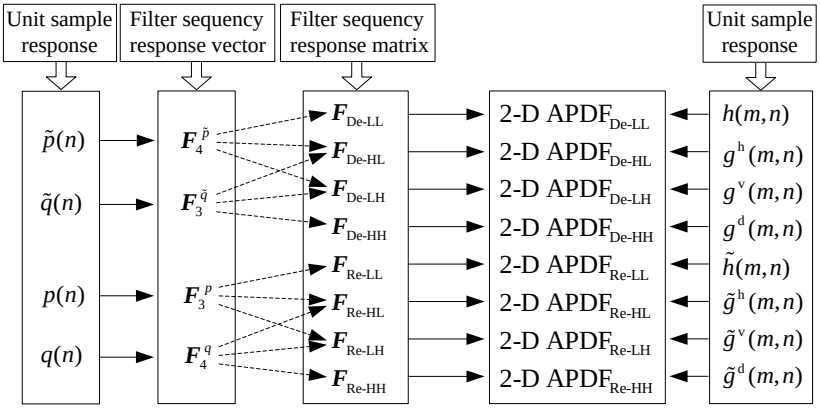

Figure 9. The Filter Sequency Response Vectors and Matrices Correspond to the 2-D APDF in 2-D Biorthogonal Wavelet Transform

In 2-D APDF based on DFT, we denote transition matrix $\boldsymbol{G}_N$ as $\left[\boldsymbol{G}_N\right]_{\text{DFT}}$. And in 2-D APDF based on IDCT, we denote transition matrix $\boldsymbol{G}_N$ as $\left[\boldsymbol{G}_N\right]_{\text{IDCT}}$.

There are some relations between frequency (sequency) response matrices (vectors) in 2-D APDF based on DFT and sequency response matrices (vectors) in 2-D APDF based on IDCT. That is

$$\begin{cases} \left[\boldsymbol{F}_{M\times N}\right]_{\text{DFT}} = \left[\boldsymbol{G}_M^{-1}\right]_{\text{DFT}}\left(\left[\boldsymbol{G}_M\right]_{\text{IDCT}}\left[\boldsymbol{F}_{M\times N}\right]_{\text{IDCT}}\left[\boldsymbol{G}_N^{\text{T}}\right]_{\text{IDCT}}\right)\left[(\boldsymbol{G}_N^{-1})^{\text{T}}\right]_{\text{DFT}} \\ \qquad\qquad = \left(\left[\boldsymbol{G}_M^{-1}\right]_{\text{DFT}}\left[\boldsymbol{G}_M\right]_{\text{IDCT}}\right)\left[\boldsymbol{F}_{M\times N}\right]_{\text{IDCT}}\left(\left[\boldsymbol{G}_N^{\text{T}}\right]_{\text{IDCT}}\left[(\boldsymbol{G}_N^{-1})^{\text{T}}\right]_{\text{DFT}}\right), \\ \left[\boldsymbol{F}_{M\times N}\right]_{\text{IDCT}} = \left[\boldsymbol{G}_M^{-1}\right]_{\text{IDCT}}\left(\left[\boldsymbol{G}_M\right]_{\text{DFT}}\left[\boldsymbol{F}_{M\times N}\right]_{\text{DFT}}\left[\boldsymbol{G}_N^{\text{T}}\right]_{\text{DFT}}\right)\left[(\boldsymbol{G}_N^{-1})^{\text{T}}\right]_{\text{IDCT}} \\ \qquad\qquad = \left(\left[\boldsymbol{G}_M^{-1}\right]_{\text{IDCT}}\left[\boldsymbol{G}_M\right]_{\text{DFT}}\right)\left[\boldsymbol{F}_{M\times N}\right]_{\text{DFT}}\left(\left[\boldsymbol{G}_N^{\text{T}}\right]_{\text{DFT}}\left[(\boldsymbol{G}_N^{-1})^{\text{T}}\right]_{\text{IDCT}}\right). \end{cases} \tag{29}$$

$$\begin{cases} \left[\boldsymbol{F}_N\right]_{\text{IDCT}} = \left[\boldsymbol{G}_N^{-1}\right]_{\text{IDCT}}\left(\left[\boldsymbol{G}_N\right]_{\text{DFT}}\left[\boldsymbol{F}_N\right]_{\text{DFT}}\right) = \left(\left[\boldsymbol{G}_N^{-1}\right]_{\text{IDCT}}\left[\boldsymbol{G}_N\right]_{\text{DFT}}\right)\left[\boldsymbol{F}_N\right]_{\text{DFT}}, \\ \left[\boldsymbol{F}_N\right]_{\text{DFT}} = \left[\boldsymbol{G}_N^{-1}\right]_{\text{DFT}}\left(\left[\boldsymbol{G}_N\right]_{\text{IDCT}}\left[\boldsymbol{F}_N\right]_{\text{IDCT}}\right) = \left(\left[\boldsymbol{G}_N^{-1}\right]_{\text{DFT}}\left[\boldsymbol{G}_N\right]_{\text{IDCT}}\right)\left[\boldsymbol{F}_N\right]_{\text{IDCT}}. \end{cases} \tag{30}$$

5. Experimental Results

The theories and methods to implement the 2-D biorthogonal wavelet transform using 2-D APDF have been described in the above sections. The biorthogonal wavelet "CDF 9/7" is selected as an example to explain the process of transformation. The typical test image "Lena" is used as a 2-D input signal to simulate the process of biorthogonal wavelet transform in computer by MATLAB7.0. If the result presents the reconstructed image well, we could draw a conclusion that 2-D APDF method can implement 2-D biorthogonal wavelet transform.

Filter sequency response vectors $\boldsymbol{F}_4^{\tilde{p}}$, $\boldsymbol{F}_3^{\tilde{q}}$, $\boldsymbol{F}_3^{p}$ and $\boldsymbol{F}_4^{q}$ shown in Table 1 ~ Table 4 can be calculated by (28). In 2-D APDF based on DFT, we denote frequency (sequency) response vectors as $\left[\boldsymbol{F}_4^{\tilde{p}}\right]_{\text{DFT}}$, $\left[\boldsymbol{F}_3^{\tilde{q}}\right]_{\text{DFT}}$, $\left[\boldsymbol{F}_3^{p}\right]_{\text{DFT}}$ and $\left[\boldsymbol{F}_4^{q}\right]_{\text{DFT}}$. And in 2-D APDF based on IDCT, we denote sequency response vectors as $\left[\boldsymbol{F}_4^{\tilde{p}}\right]_{\text{IDCT}}$, $\left[\boldsymbol{F}_3^{\tilde{q}}\right]_{\text{IDCT}}$, $\left[\boldsymbol{F}_3^{p}\right]_{\text{IDCT}}$ and $\left[\boldsymbol{F}_4^{q}\right]_{\text{IDCT}}$.

Table 1. Frequency (Sequency) Response Vectors in 2-D APDF based on DFT Corresponding to Decomposition Filters

Vector index n	Frequency (sequency) response vectors in 2-D APDF based on DFT	
	$\left[\boldsymbol{F}_4^{\tilde{p}}\right]_{\mathrm{DFT}}$	$\left[\boldsymbol{F}_3^{\tilde{q}}\right]_{\mathrm{DFT}}$
0	1.269596856148298 + 0.000000000000000i	-0.407805947406553 + 0.000000000000000i
1	1.254324988807367 - 0.195452897915145i	-0.869864451623911 - 0.815611894810278i
2	0.242623280640718 - 0.284759377903535i	-1.006407614967956 + 0.000000000000000i
3	0.242623280640718 + 0.284759377903535i	-0.869864451623911 + 0.815611894810278i
4	1.254324988807368 + 0.195452897915146i	

Table 2. Frequency (Sequency) Response Vectors in 2-D APDF based on DFT Corresponding to Reconstruction Filters

Vector index n	Frequency (sequency) response vectors in 2-D APDF based on DFT	
	$\left[\boldsymbol{F}_3^{p}\right]_{\mathrm{DFT}}$	$\left[\boldsymbol{F}_4^{q}\right]_{\mathrm{DFT}}$
0	1.006407614967956 + 0.000000000000000i	-0.445337042214006 + 0.000000000000000i
1	0.869864451623911 - 0.815611894810278i	-0.866292135994508 - 0.771967533900112i
2	0.407805947406553 + 0.000000000000000i	-1.042786040420724 - 0.156409258267169i
3	0.869864451623911 + 0.815611894810278i	-1.042786040420724 + 0.156409258267169i
4		-0.866292135994508 + 0.771967533900112i

Table 3. Sequency Response Vectors in 2-D APDF based on IDCT Corresponding to Decomposition Filters

Vector index n	Sequency response vectors in 2-D APDF based on IDCT	
	$\left[\boldsymbol{F}_4^{\tilde{p}}\right]_{\mathrm{IDCT}}$	$\left[\boldsymbol{F}_3^{\tilde{q}}\right]_{\mathrm{IDCT}}$
0	1.428286805837736	0.072222484285374
1	1.332914285689320	-0.171634138799509
2	1.444197632013266	-1.596019565934742
3	0.139929130748674	-1.458511245173454
4	-0.081834459244526	

Table 4. Sequency Response Vectors in 2-D APDF based on IDCT Corresponding to Reconstruction Filters

Vector index n	Sequency response vectors in 2-D APDF based on IDCT	
	$\left[\boldsymbol{F}_3^{p}\right]_{\mathrm{IDCT}}$	$\left[\boldsymbol{F}_4^{q}\right]_{\mathrm{IDCT}}$
0	1.458511245173454	0.081834459244526
1	1.596019565934743	-0.139929130748674
2	0.171634138799509	-1.444197632013266
3	-0.072222484285374	-1.332914285689320
4		-1.428286805837736

With sequency response vectors $\boldsymbol{F}_4^{\tilde{p}}$, $\boldsymbol{F}_3^{\tilde{q}}$, $\boldsymbol{F}_3^{p}$ and $\boldsymbol{F}_4^{q}$, the sequency response matrices $\boldsymbol{F}_{\text{De-LL}}$, $\boldsymbol{F}_{\text{De-HL}}$, $\boldsymbol{F}_{\text{De-LH}}$, $\boldsymbol{F}_{\text{De-HH}}$ and $\boldsymbol{F}_{\text{Re-LL}}$, $\boldsymbol{F}_{\text{Re-HL}}$, $\boldsymbol{F}_{\text{Re-LH}}$, $\boldsymbol{F}_{\text{Re-HH}}$ in 2-D APDF can be obtained according to (26) and (27). Therefore, $\left[\boldsymbol{F}_{\text{De-LL}}\right]_{\text{DFT}}$, $\left[\boldsymbol{F}_{\text{De-HL}}\right]_{\text{DFT}}$, $\left[\boldsymbol{F}_{\text{De-LH}}\right]_{\text{DFT}}$, $\left[\boldsymbol{F}_{\text{De-HH}}\right]_{\text{DFT}}$, $\left[\boldsymbol{F}_{\text{Re-LL}}\right]_{\text{DFT}}$, $\left[\boldsymbol{F}_{\text{Re-HL}}\right]_{\text{DFT}}$, $\left[\boldsymbol{F}_{\text{Re-LH}}\right]_{\text{DFT}}$, $\left[\boldsymbol{F}_{\text{Re-HH}}\right]_{\text{DFT}}$ and $\left[\boldsymbol{F}_{\text{De-LL}}\right]_{\text{IDCT}}$, $\left[\boldsymbol{F}_{\text{De-HL}}\right]_{\text{IDCT}}$, $\left[\boldsymbol{F}_{\text{De-LH}}\right]_{\text{IDCT}}$, $\left[\boldsymbol{F}_{\text{De-HH}}\right]_{\text{IDCT}}$, $\left[\boldsymbol{F}_{\text{Re-LL}}\right]_{\text{IDCT}}$, $\left[\boldsymbol{F}_{\text{Re-HL}}\right]_{\text{IDCT}}$, $\left[\boldsymbol{F}_{\text{Re-LH}}\right]_{\text{IDCT}}$, $\left[\boldsymbol{F}_{\text{Re-HH}}\right]_{\text{IDCT}}$ can be calculated. Then 2-D biorthogonal wavelet transform will be realized using 2-D APDF based on DFT and 2-D APDF based on IDCT. What's more, the relations between (29) and (30) are verified by calculation result of sequency response vectors and matrices in 2-D APDF based on DFT and IDCT.

The amplitude-frequency responses of four 2-D decomposition filters designed by 2-D APDF method are shown in Figure 10, which are used to dispose 2-D signals. Reconstruction filters are shown in Figure 11. The 2-D decomposition and reconstruction filters in 2-D APDF based on DFT and IDCT are identical.

The multi-level decomposition and reconstruction are not the focus of this paper, so we take only one layer biorthogonal wavelet transform to illustrate the feasibility of the proposed algorithm. Here we only give the one layer biorthogonal wavelet decomposition and reconstruction results of the test image "Lena.bmp" with size of 512×512. The result is displayed in Figure 12 and Figure 13.

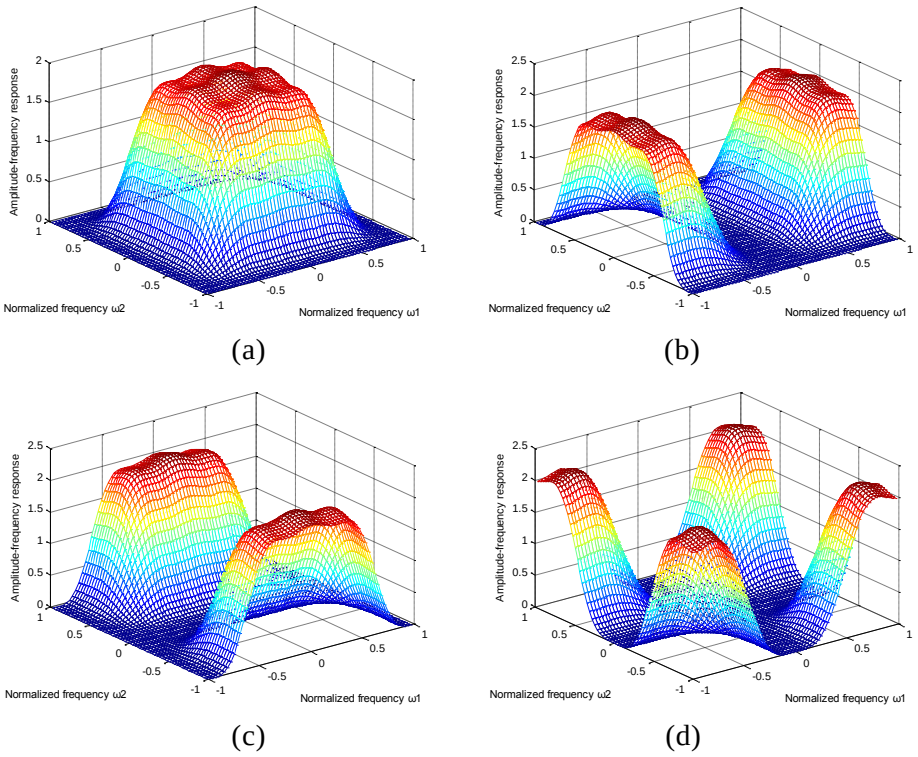

Figure 10. The Three-dimensional Perspectives of Amplitude-frequency Responses of 2-D APDF used to Decompose 2-D Signals: (a) Low-pass Filter, (b) Horizontal High-pass Filter, (c) Vertical High-pass Filter, (d) Diagonal High-pass Filter

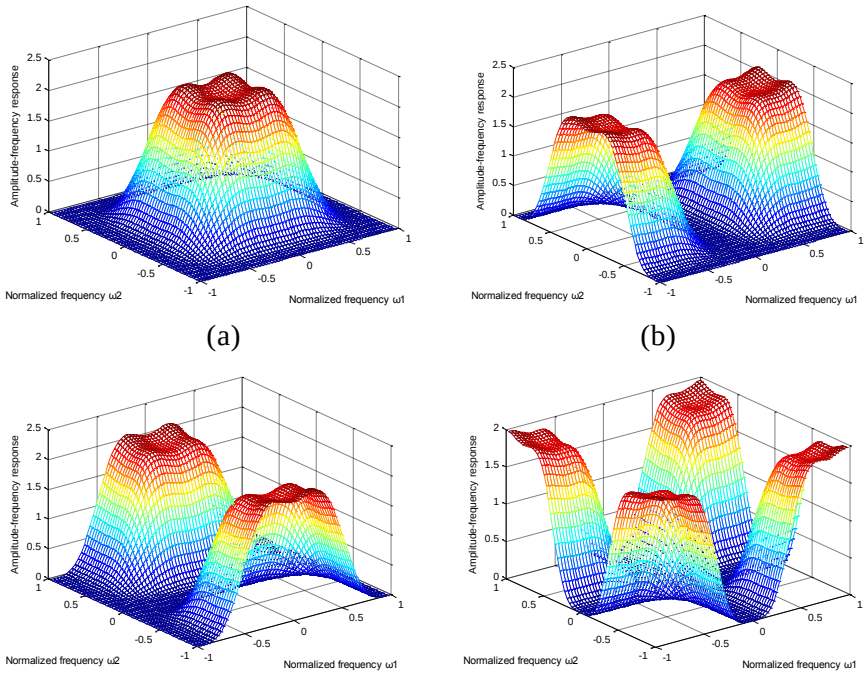

Figure 11. The Three-dimensional Perspectives of Amplitude-frequency Responses of 2-D APDF used to Reconstruct 2-D Signals: (a) Low-pass Filter, (b) Horizontal High-pass Filter, (c) Vertical High-pass Filter, (d) Diagonal High-pass Filter

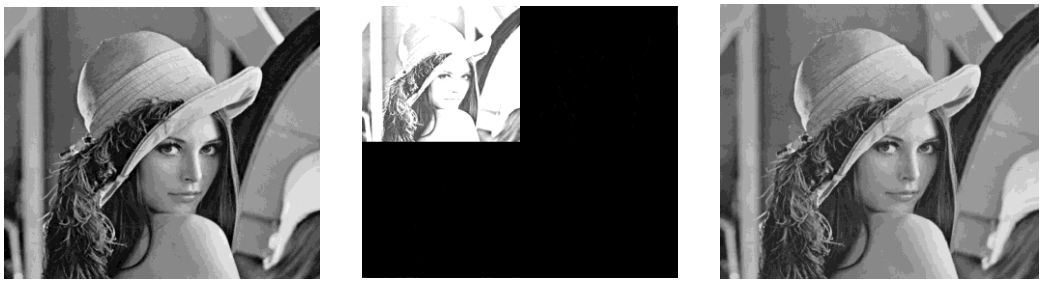

Figure 12. The Decomposition and Reconstruction Results using 2-D APDF based on DFT: (a) Original Image, (b) Decomposition, (c) Reconstruction

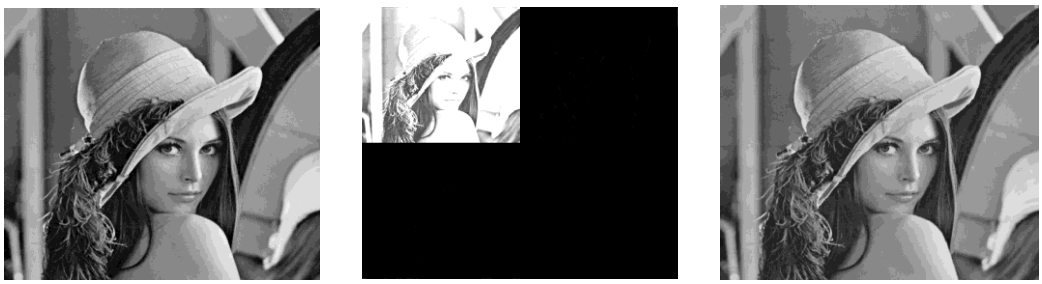

Figure 13. The Decomposition and Reconstruction Results using 2-D APDF based on IDCT: (a) Original Image, (b) Decomposition, (c) Reconstruction

In addition, we also adopt the mean squared error (MSE) to evaluate the success of the implementation. After the processes of decomposition and reconstruction, the value of MSE is 4.2039×10^{-22} by applying 2-D APDF based on DFT, and the value of MSE is 4.1762×10^{-22} by applying 2-D APDF based on IDCT. These results are very close to zero. In other words, we achieve 2-D biorthogonal wavelet transform using 2-D APDF. On the other hand, sequency response vectors in 2-D APDF based on IDCT always are real vectors, which make it more convenient to achieve 2-D biorthogonal wavelet transform using 2-D APDF based on IDCT.

6. Conclusion

This paper proposes a new algorithm to implement 2-D biorthogonal wavelet transform using the 2-D APDF. We have done experiments in MATLAB7.0. 2-D APDF is applied in processing test images. Experimental results show that the results of decomposition and reconstruction perform very well and values of MSE are close to zero. So we have ample reasons to support that 2-D biorthogonal wavelet transform can be implemented using 2-D APDF. Furthermore, the relations between frequency (sequency) response matrices (vectors) in 2-D APDF based on DFT and sequency response matrices (vectors) in 2-D APDF based on IDCT are discussed. Although APDF based on DFT has some advantages in performance of filtering compared with APDF based on IDCT, it is more convenient to achieve 2-D biorthogonal wavelet transform using 2-D APDF based on IDCT.

For further work, we can apply 2-D filters designed through 2-D APDF based on DFT method to the applications of digital image processing such as image coding, image denoising, etc. 2-D windowed APDF based on DCT, IDCT and DFT are also deserved exploration and applied to many fields.

Acknowledgements

This work was supported by the National Natural Science Foundation of China (Grant No. 61201371) and the promotive research fund for excellent young and middle-aged scientists of Shandong Province, China (Grant No. BS2013DX022). The authors would like to thank Fanfan Yang, Xiaoyan Wang, and Ran Wei for their kind help and valuable suggestions. The authors also thank the anonymous reviewers and the editors for their valuable comments to improve the presentation of the paper.

References

[1] W. Lu and A. Antonious, "Two-Dimensional Digital Filters", Marcel Dekker, Inc., New York, **(1992)**.
[2] C. Charalambous, "Design of *N*-dimensional multiplierless spherically symmetric FIR digital filters by transformation", IEE Proceedings G, Electronic Circuits and Systems, vol. 135, no. 5, **(1988)**, pp. 203-210.
[3] P. A. Stubberud, "2-D linear phase frequency sampling filters and 2-D linear phase frequency sampling filters with fourfold symmetry", in: Proc. of the IEEE International Symposium on Circuits and Systems, Atlanta, GA, USA, **(1996)**, pp. 356-359.
[4] Z. X. Hou, Z. H. Wang and X. Yang, "Design and implementation of all phase DFT digital filter", Acta Electronica Sinica, vol. 31, no. 4, **(2003)**, pp. 539-543. (in Chinese)
[5] F. Su and Z. H. Wang, "Implementation and design of all phase FIR filter in DCT domain", Journal of Tianjin University (Science and Technology), vol. 37, no. 12, **(2004)**, pp. 1110-1114. (in Chinese)
[6] L. L. Zhao, "All phase digital filtering and image interpolation based on IDCT/DCT", Ph.D. Thesis, Tianjin University, China, **(2006)**, pp. 20-22, 49-58. (in Chinese)
[7] S. G. Mallat, "Multiresolution approximations and wavelet orthonormal bases of $\boldsymbol{L}^2(\boldsymbol{R})$", Trans. of the American Mathematical Society, vol. 315, no. l, **(1989)**, pp. 69-87.
[8] D. L. Donoho, "De-noising by soft-thresholding", IEEE Trans. on Information Theory, vol. 41, no. 3, **(1995)**, pp. 613-627.

[9] S. L. Mei, "HPM-based dynamic wavelet transform and its application in image denoising", Mathematical Problems in Engineering, vol. 2013, Article ID 309418, **(2013)**, pp. 1-10.
[10] D. Taubman, "High performance scalable image compression with EBCOT", IEEE Trans. on Image Processing, vol. 9, no. 7, **(2000)**, pp. 1158-1170.
[11] S. G. Mallat, "A theory for multiresolution signal decomposition: the wavelet representation", IEEE Trans. on Pattern Analysis and Machine Intelligence, vol. 11, no. 7, **(1989)**, pp. 674-693.
[12] B. C. Jiang, A. P. Yang, C. Y. Wang, and Z. X. Hou, "Implementation of biorthogonal wavelet transform using discrete cosine sequency filter", International Journal of Signal Processing, Image Processing and Pattern Recognition, vol. 6, no. 4, **(2013)**, pp. 179-189.
[13] W. Sweldens, "The lifting scheme: A construction of second generation wavelets", SIAM Journal on Mathematical Analysis, vol. 29, no. 2, **(1998)**, pp. 511-546.
[14] S. G. Mallat, "A Wavelet Tour of Signal Processing", Academic Press, San Diego, **(1998)**, pp. 220-321.
[15] C. Y. Wang, "Research on all phase biothogonal transform theory and its applications in image coding", Ph.D. Thesis, Tianjin University, China, **(2010)**, pp. 25-28, 106-114. (in Chinese)
[16] Z. H. Wang and X. D. Huang, "All Phase Spectrum Analysis and Filtering Techniques for Digital Signal", Publishing House of Electronics Industry, Beijing, China, **(2009)**, pp. 1-8. (in Chinese)
[17] Z. X. Hou, "Design and implementation of the all phase sequency filter", Signal Processing, vol. 17, supplement, **(2001)**, pp. 132-135. (in Chinese)
[18] L. L. Zhao and Z. X. Hou, "Windowed all phase digital filter based on IDCT", Journal of Tianjin University (Science and Technology), vol. 39, no. 12, **(2006)**, pp. 1499-1503. (in Chinese)
[19] Z. X. Hou, "Design and application of the discrete cosine sequency filters", Journal of Tianjin University (Science and Technology), vol. 32, no. 3, **(1999)**, pp. 324-328. (in Chinese)
[20] Z. X. Hou, "A convolution algorithm for discrete cosine sequency filtering", Journal of China Institute of Communications, supplement, vol. 20, **(1999)**, pp. 211-215. (in Chinese)

Authors

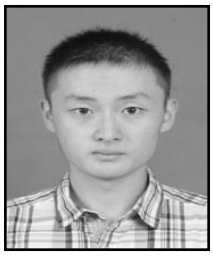

Qiming Fu, was born in Jiangxi province, China in 1992. He received his B.S. degree in electronic information science and technology from Shandong University, Weihai, China in 2013. He is currently pursuing his M.E. degree in electronics and communication engineering in Shandong University, Weihai, China. His current research interests include digital image processing and transmission technology.

Xiao Zhou, was born in Shandong province, China in 1982. She received her B.E. degree in automation from Nanjing University of Posts and Telecommunications, China in 2003, her M.E. degree in information and communication engineering from Inha University, Korea in 2005, and her Ph.D. degree in information and communication engineering from Tsinghua University, China in 2013. Now she is a lecturer in the School of Mechanical, Electrical and Information Engineering, Shandong University, Weihai, China. Her current research interests include wireless communication technology, digital image processing and analysis.

Chengyou Wang, was born in Shandong province, China in 1979. He received his B.E. degree in electronic information science and technology from Yantai University, China in 2004, and his M.E. and Ph.D. degree in signal and information processing from Tianjin University, China in 2007 and 2010 respectively. Now he is an associate professor in the School of Mechanical, Electrical and Information Engineering, Shandong University, Weihai, China. His current research interests include digital image & video processing and analysis, multidimensional signal and information processing.

Baochen Jiang, was born in Shandong province, China in 1962. He received his B.S. degree in radio electronics from Shandong University, China in 1983, and his M.E. degree in communication and electronic systems from Tsinghua University, China in 1990. Now he is a professor in the School of Mechanical, Electrical and Information Engineering, Shandong University, Weihai, China. His current research interests include signal and information processing, image & video processing, and smart grid technology.